

## Use of a portable topographic mapping millimetre wave radar at an active lava flow

D. G. Macfarlane,<sup>1</sup> G. Wadge,<sup>2</sup> D. A. Robertson,<sup>1</sup> M. R. James,<sup>3</sup> and H. Pinkerton<sup>3</sup>

Received 19 October 2005; revised 8 December 2005; accepted 13 December 2005; published 1 February 2006.

[1] A ground-based millimetre wave radar, AVTIS (All-weather Volcano Topography Imaging Sensor), has been developed for topographic monitoring. The instrument is portable and capable of measurements over ranges up to  $\sim 7$  km through cloud and at night. In April and May 2005, AVTIS was deployed at Arenal Volcano, Costa Rica, in order to determine topographic changes associated with the advance of a lava flow. This is the first reported application of mm-wave radar technology to the measurement of lava flux rates. Three topographic data sets of the flow were acquired from observation distances of  $\sim 3$  km over an eight day period, during which the flow front was detected to have advanced  $\sim 200$  m. Topographic differences between the data sets indicated a flow thickness of  $\sim 10$  m, and a dense rock equivalent lava flux of  $\sim 0.20 \pm 0.08 \text{ m}^3 \text{ s}^{-1}$ . **Citation:** Macfarlane, D. G., G. Wadge, D. A. Robertson, M. R. James, and H. Pinkerton (2006), Use of a portable topographic mapping millimetre wave radar at an active lava flow, *Geophys. Res. Lett.*, *33*, L03301, doi:10.1029/2005GL025005.

### 1. Introduction

[2] Topographic measurements are critical to a wide range of scientific and hazard monitoring applications. In many cases, changes in topography are relatively small and occur sufficiently slowly that accurate measurements can be carried out using conventional or spaceborne surveying methods. In other cases (e.g., large landslips, lava flows or dome growth at volcanoes) changes can be rapid, creating conditions under which only remote sensing can be employed safely. In these instances suitable techniques such as ground-based laser ranging [Hunter *et al.*, 2003], airborne lidar [Mazzarini *et al.*, 2005] and photogrammetry [Baldi *et al.*, 2005] are reliant on good visibility (e.g., no obscuration by cloud, fog or condensing volcanic gases). Such cases require the use of radar techniques (e.g., radar interferometry [Lu *et al.*, 2003]), however the timely application of traditional radar methods can be restricted by aircraft availability or the frequency of satellite repeat passes. Furthermore, radar interferometry fails on rapidly evolving surfaces such as active lava domes due to the decorrelation of returns [Wadge *et al.*, 1999]. Consequently, existing radar systems are not usually suitable for reliable and timely hazard assessment on volcanoes.

<sup>1</sup>School of Physics and Astronomy, University of St Andrews, Fife, UK.

<sup>2</sup>Environmental Systems Science Centre, University of Reading, Reading, UK.

<sup>3</sup>Lancaster Environment Centre, Lancaster University, Lancaster, UK.

[3] The AVTIS (All-weather Volcano Topography Imaging Sensor) radar was designed to fulfill this requirement by providing a compact, portable unit that can easily be deployed in the field [Wadge *et al.*, 2006a, 2006b]. This is achieved by operating in the millimetre wave band of the electromagnetic spectrum. For the same size of antenna, mm-waves provide inherently higher angular resolution than can be achieved with the longer wavelengths of traditional microwave radar while retaining the advantage of low attenuation through cloud. The instrument can therefore produce high spatial resolution measurements continuously through conditions of no visibility. Other high performance mm-wave radars exist but they tend to have been optimised for very different applications (e.g., runway debris detection [Beasley *et al.*, 2004]) and are not well suited for topographic surveying. For environments prone to conditions of poor visibility AVTIS represents a valuable advance in our long-range measurement capability.

[4] The results of an initial AVTIS deployment on Montserrat [Wadge *et al.*, 2006a, 2006b] illustrated the potential of the instrument for topographic monitoring. Subsequent significant advances in hardware and data processing have improved the signal to noise ratio by 27 dB extending our maximum detection range from 3.8 km to  $\sim 7$  km with a range resolution of  $\sim 1$  m. Consequently, localised topographic changes can now be easily detected. Here we present data from Arenal volcano, Costa Rica, which demonstrate the usefulness of AVTIS as a tool for remotely monitoring active lava flows.

[5] This application is driven by a requirement to improve our ability to measure the rate at which lava is erupted from volcanoes; a critical parameter that is often very difficult to measure directly due to factors such as hazardous conditions and problems of access. This is the case at Arenal, where effusion rate estimates have been carried out previously using low repeat-frequency remote topographic measurements [Wadge, 1983; Wadge *et al.*, 2006a, 2006b]. Under conditions where close approach is possible and safe, then methods of estimating effusion rate such as measuring very low frequency electromagnetic fields [Kauahikaua *et al.*, 1996] can be used. Radiant heat flux measurements can also be used as a mass flux rate proxy [e.g., Calvari *et al.*, 2005]. Our AVTIS measurements were carried out in April and May 2005, when small, low-effusion rate basaltic andesite lava flows were descending from the summit vents.

### 2. Millimetre Wave Topographic Imaging

[6] The AVTIS instrument is a portable, tripod-mounted, 94 GHz FMCW mm-wave radar unit designed for ground-based deployment around active volcanoes. The radar consists of a single transmit/receive antenna and radar head (on

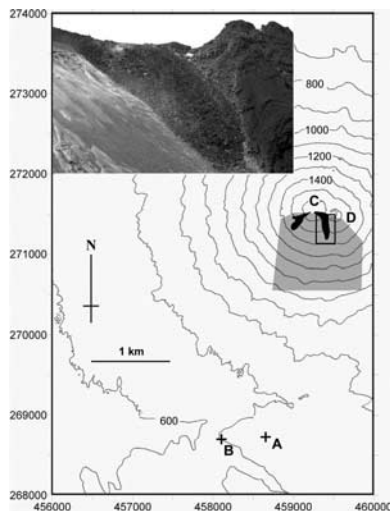


**Figure 1.** Map of Arenal Volcano (100 m contours, Costa Rican national grid in metres) with the new and old summit cones labelled C and D respectively. The two active lava flows of April/May 2005 are shown in black. The AVTIS radar imaged the southern lava flow between cones C and D from sites A and B. The outline rectangle represents the area around this flow shown in detail in Figure 2. The inset photograph shows the view of the flow from A on 1 May, during a period of exceptional visibility. The peaks observed on the right of the image represent the older eastern summit cone D.

a pan and tilt gimbal), a power supply unit, batteries and a laptop. For technical details, see Macfarlane and Robertson [2004, 2005].

[7] An angular raster scan of the radar across a scene gives a volume data set of backscattered power against range for the azimuth and elevation values covered. In order to extract topographic information (i.e., the appropriate range values), a ‘surface indicator’ criterion has to be applied for each line of sight. In many conventional radar applications, the aim is to identify a reflective point-like (sub-beamwidth) target at a specific range against a background level of clutter. The target range is indicated by the range bin containing return power above a certain threshold [Skolnik, 1990]. However, when trying to measure the range to beam-filling natural topography, the clutter itself becomes the target. The radar return signal is produced by an ensemble of individual point scatterers of similar reflectivity (such as angular rocks) contained within the extended radar footprint and is typically spread in range. Using a simple power threshold criterion on the raw power spectra results in a high degree of noise within the surface data. Consequently, we have introduced a

series of data processing steps to improve surface determination when imaging natural topography. These are: (i) power versus range normalisation, (ii) low pass filtering, (iii) maximum power detection, and finally, (iv) power thresholding.

[8] The initial normalisation corrects the data for the  $(1/\text{range})^2$  fall-off in reflected power associated with beam-filling targets [Skolnik, 1990]. The normalised data are then filtered with a low pass 50-bin two-way (phase invariant) filter. This significantly reduces the noise from point scatterers but leaves the range to the maximum signal return unaltered, producing a range spectrum that represents the average distance to the illuminated surface. Range is then indicated by the bin of maximum power return in the filtered spectrum (step iii). Finally, false returns (e.g., lines of sight to clear air) are detected and removed by comparison with a power threshold based on a Gaussian fit to the overall distribution of maximum power return from the entire raster data set. For the data presented here, a threshold value of 2.0 sigma was used.

[9] The resultant data points have polar co-ordinates of azimuth, elevation and range. With knowledge of the radar position and pointing direction, these are converted into Cartesian co-ordinates and a digital elevation model (DEM) can then be constructed by interpolating surface height over an x-y grid of selected resolution.

### 3. Measurements at Arenal

[10] During late April to early May 2005, two lava flows were observed erupting from vents at the summit of the volcano ( $\sim 1700$  m a.s.l., Figure 1). One flow descended the steep slopes of the upper cone to the southwest and largely disintegrated into rockfalls on the upper slopes. Another moved eastward to the col separating the old and new cones before turning southward. Our measurements of this second flow from two observing sites A and B (Figure 1), about 3 km to the south and south-southwest respectively, are presented here (Table 1). On 23 April, the flow was visible, although atmospheric haze and intermittent cloud obscured details and would have prevented the use of other remote sensing methods such as photogrammetry or laser scanning. On 27 April, observations were carried out in the evening, with the majority of the data collected during darkness. The restricted glow from rock-fall activity on the upper slopes of the volcano indicated that cloud also covered the summit and lava flow regions. The final 1 May acquisition provided good visibility of the flow and allowed the photograph shown in Figure 1 to be taken.

[11] At location A (occupied on 27 April and 1 May), an existing permanent instrument mounting at the Arenal

**Table 1.** Data Acquisition Details

Date	Location	Range to Lava Flow	Coarse Scans (0.25° Sampling Interval)			Fine Scans (0.05° Sampling Interval)		
			Start Time, LT	Duration	Angular Area (Azimuth × Elevation)	Start Time, LT	Duration	Angular Area (Azimuth × Elevation)
23/04/05	B	3000 m	09:00	20 min	20.0° × 5.5°	08:50	80 min	20.0° × 3.0°
27/04/05	A	2800 m	16:35	75 min	37.5° × 13.0°	18:10	60 min	13.0° × 2.5°
01/05/05	A	2800 m	16:25	55 min	35.5° × 12.75°	10:45	60 min	8.5° × 3.6°

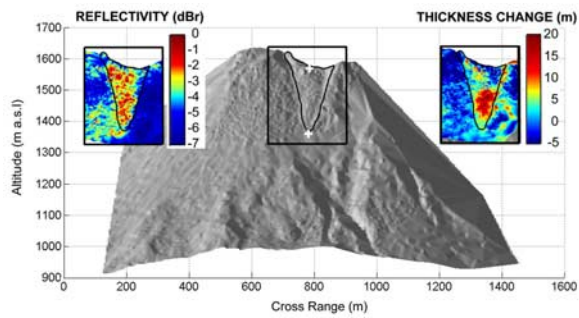


**Figure 2.** The main image is of shaded topography on the south side of Arenal Volcano measured by AVTIS from site A on 1 May 2005. The active lava flow is outlined in black. The left inset shows how the reflectivity of the surface (returned radar power, in dB, relative to the maximum return in the image) discriminates well between lava (red) and ash (blue). The right inset shows the increase in thickness of the lava flow in metres between 23 April and 1 May 2005. The white crosses mark the start and end points of the profile cut shown in Figure 3.

Observatory Lodge was used to site the radar. At location B (occupied on 23 May), AVTIS was mounted on a surveying tripod whose position was determined by dGPS. At each site, the entire view of the volcano was imaged at a coarse angular increment of  $0.25^\circ$  with an additional scan of the summit (including the lava flow) at a finer increment of  $0.05^\circ$ .

[12] Whilst the threaded instrument mount at A gave a fixed spatial position for the radar, it did not provide perfect angular re-alignment between the two days. Alignment by observation of a control point corner cube was also prevented by the local topography and close proximity of trees at this site. Hence, to improve the data registration, an area of no topographic change common to both DEMs was selected and a local search of azimuth-elevation space was carried out to find the angular offsets that minimised the rms differences between the two surfaces. A similar procedure was carried out to align data from site B; an initial radar orientation determined by imaging corner cube control points co-ordinated by dGPS [Wadge *et al.*, 2006a, 2006b] was then improved by minimising surface differences. Finally, in order to accommodate minor remaining uncertainties in the relative radar imaging orientations between sites A and B, an iterative closest point refinement (a standard technique for merging laser scanner data) was carried out. This refinement was responsible for adjusting point co-ordinates by only  $\sim 2$  m. After registration the data sets were interpolated to a common horizontal grid (of spacing 2.5 m) for direct comparison.

[13] The AVTIS-derived DEM of the southern side of Arenal acquired on 1 May is shown in Figure 2 as projected shaded relief. Although the topographic representation appears to be reasonable, some surface noise is apparent. Differencing the registered DEMs for 23 April, 27 April and 1 May reveals the vertical changes over the intervening periods. Between 23 April and 1 May, an area of positive height change, with an average value of  $\sim 10$  m and maximum values of  $\sim 20$  m, was measured at the distal end of the lava flow (Figure 2, top right inset, and Figure 3).

This area corresponds to an advance of  $\sim 200$  m for the flow over the eight days.

#### 4. Discussion

[14] Although the differenced topography in Figure 2 clearly shows the advancing flow, there are other areas of apparent topographic change of  $\pm 5$  m which are not correlated with real topographic variation. This relatively high frequency ‘noise’ is believed to be a remnant effect of strong, discrete point scatterers which have not been completely removed by the low-pass filtering. For a target slope of  $\sim 30^\circ$ , at range of 3000 m and viewed from an elevation angle of  $\sim 16^\circ$ , an apparent height error of  $\pm 7$  m would be given if the return signal was dominated by a point scatterer located either at the top or the bottom of the main lobe. If the beam was in identical orientations during repeat observations, then this effect would not be detected as a topographic difference during analysis. However, with the instrument removed between observations, precise realignment was not possible and therefore strong permanent scatterers may be represented differently within the data sets.

[15] Analogous to laser scanner data, each topographic point determined by AVTIS is accompanied by a power value describing the strength of the returned signal. Lava flows are renowned for being highly reflective surfaces for microwave radars [Plaut *et al.*, 2004] due to their local surface roughness, and the lava flows of Arenal are typically blocky [Borgia *et al.*, 1983], so should provide strong edge, point and facet reflectors. This is the case for the lava flow imaged here (Figure 2, top left inset), which is significantly more reflective than the surrounding surfaces which were generally dominated by ash and small clasts.

[16] The surface-to-surface topographic changes detected in the area of the lava flow can be converted to volumetric flux rates by dividing by the appropriate time intervals. The rate between 23 and 27 April is  $0.29 \pm 0.15 \text{ m}^3 \text{ s}^{-1}$ , between 27 April and 1 May is  $0.16 \pm 0.08 \text{ m}^3 \text{ s}^{-1}$  and overall, between 23 April and 1 May is  $0.23 \pm 0.1 \text{ m}^3 \text{ s}^{-1}$  (or  $0.20 \pm 0.08 \text{ m}^3 \text{ s}^{-1}$ , when converted to dense rock equivalent ( $\times 0.86$ )). The uncertainties were calculated from the area of no topographic change used in the registration process. The

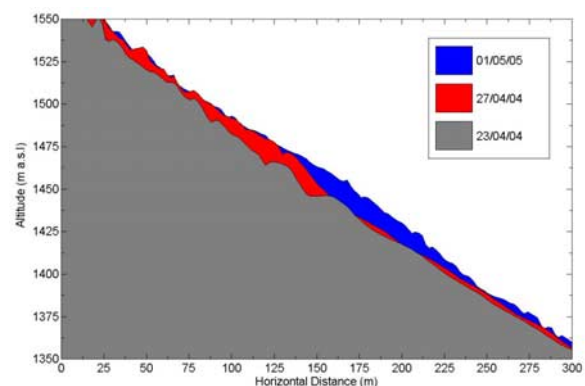


**Figure 3.** True scale vertical profile down the lava flow shown in Figure 2 showing the changes in the surfaces measured by AVTIS on 23, 27 April, and 1 May 2005 as the lava flow advanced.

vent and proximal parts of the flow were not observable from A or B, so we cannot determine how closely these measured rates reflect the actual vent effusion rate. Factors such as channel drainage of a flow that is not being actively fed at the time [Borgia *et al.*, 1984] cannot be discounted.

[17] The observed rates on Arenal during April and May 2005 are low, both in terms of Arenal's long-term behaviour since 1968 [Wadge *et al.*, 2006a, 2006b] and in comparison to many other lava flow eruptions at other volcanoes, where effusion rates of  $0.1\text{--}10\text{ m}^3\text{s}^{-1}$  are the norm.

[18] Our measurements of Arenal's 2005 activity were made under relatively favourable viewing conditions (i.e., a large fraction of volume change was accounted for by apparent surface motion along the radar line of sight). The changes were also detected from different locations with less favourable (more oblique) observation angles but the calculations associated with these measurements are consequently prone to larger errors. A full discussion of this issue is left for future work, nevertheless we have demonstrated the ability of mm-wave radar imaging to measure topographic changes associated with low effusion rate lava flows, from different viewing points and during periods of low or no visibility.

[19] **Acknowledgments.** Eliecer Duarte and Eric Fernandez of OVSI-CORI-UNA were generous with their time and assistance with the fieldwork. We thank Mauricio Mora for his help with clearing equipment through customs. We are grateful to Paul Cole and Deliomara Oramas Dorta of Coventry University for their loan of dGPS equipment. Comments by Dave Schneider and an anonymous referee improved the paper. This work was supported by a NERC grant: NER/A/S/2001/01001.

## References

- Baldi, P., M. Fabris, M. Marsella, and R. Monticelli (2005), Monitoring the morphological evolution of the Sciara del Fuoco during the 2002–2003 Stromboli eruption using multi-temporal photogrammetry, *ISPRS J. Photogramm. Rem. Sens.*, *59*, 199–211.
- Beasley, P. D. L., G. Binns, R. D. Hodges, and R. J. Badley (2004), Tarsier<sup>®</sup>, a millimetre wave radar for airport runway debris detection, paper presented at European Radar Conference 2004, Eur. Microwave Assoc., Amsterdam.
- Borgia, A., S. Linneman, D. Spencer, L. Diego Morales, and J. Brenes Andre (1983), Dynamics of lava flow fronts, Arenal Volcano, Costa Rica, *J. Volcanol. Geotherm. Res.*, *19*, 303–329.
- Calvari, S., L. Spampinato, L. Lodato, A. J. L. Harris, M. R. Patrick, J. Dehn, M. R. Burton, and D. Andronico (2005), Chronology and complex volcanic processes during the 2002–2003 flank eruption at Stromboli volcano (Italy) reconstructed from direct observations and surveys with a handheld thermal camera, *J. Geophys. Res.*, *110*, B02201, doi:10.1029/2004JB003129.
- Hunter, G., H. Pinkerton, R. Airey, and S. Calvari (2003), The application of a long-range laser scanner for monitoring volcanic activity on Mount Etna, *J. Volcanol. Geotherm. Res.*, *123*, 203–210.
- Kauahikaua, J., M. Mangan, C. Heliker, and T. Mattox (1996), A quantitative look at the demise of a basaltic vent: The death of Kupaianaha, Kilauea volcano, Hawaii, *Bull. Volcanol.*, *57*, 641–648.
- Lu, Z., E. Fielding, M. R. Patrick, and C. M. Trautwein (2003), Estimating lava volume by precision combination of multiple baseline spaceborne and airborne interferometric synthetic aperture radar: The 1997 eruption of Okmok Volcano, Alaska, *IEEE Trans. Geosci. Remote. Sens.*, *41*, 1428–1436.
- Macfarlane, D. G., and D. A. Robertson (2004), A 94 GHz dual-mode active/passive imager for remote sensing, *Proc. SPIE Int. Soc. Opt. Eng.*, *5619*, 70–81.
- Macfarlane, D. G., and D. A. Robertson (2005), Long range, high resolution 94 GHz FMCW imaging radar (AVTIS), paper presented at Joint 30th International Conference on Infrared and Millimeter Waves and 13th International Conference on Terahertz Electronics, IEEE Microwave Theory and Tech. Soc., Williamsburg, Va.
- Mazzarini, F., M. T. Pareschi, M. Favalli, I. Isola, S. Tarquini, and E. Boschi (2005), Morphology of basaltic lava channels during the Mt. Etna September 2004 eruption from airborne laser altimeter data, *Geophys. Res. Lett.*, *32*, L04305, doi:10.1029/2004GL021815.
- Plaut, J. L., S. W. Anderson, D. A. Crown, E. R. Stofan, and J. J. van Zyl (2004), The unique radar properties of silicic lava domes, *J. Geophys. Res.*, *109*, E03001, doi:10.1029/2002JE002017.
- Skolnik, M. I. (1990), *Radar Handbook*, 2nd ed., McGraw-Hill, New York.
- Wadge, G. (1983), The magma budget of Volcan Arenal, Costa Rica from 1968 to 1980, *J. Volcanol. Geotherm. Res.*, *19*, 281–302.
- Wadge, G., B. Scheuchl, N. F. Stevens, D. A. Rothery, S. Blake, M. D. Palmer, C. Riley, and A. Smith (1999), ERS SAR interferometry of an erupting volcano on a tropical island: Soufrière Hills Volcano, Montserrat, in *Proceedings of IGARSS'99*, pp. 2170–2172, IEEE Press, Piscataway, N. J.
- Wadge, G., D. G. Macfarlane, D. A. Robertson, A. J. Hale, H. Pinkerton, R. V. Burrell, G. E. Norton, and M. R. James (2006a), AVTIS: A novel millimetre-wave ground based instrument for volcano remote sensing, *J. Volcanol. Geotherm. Res.*, *146*, 307–318.
- Wadge, G., D. Oramas Dorta, and P. D. Cole (2006b), The magma budget of Volcan Arenal, Costa Rica from 1980 to 2004, *J. Volcanol. Geotherm. Res.*, in press.
- M. R. James and H. Pinkerton, Lancaster Environment Centre, Lancaster University, Lancaster LA1 4YW, UK.
- D. G. Macfarlane and D. A. Robertson, School of Physics and Astronomy, University of St Andrews, Fife KY16 9SS, UK. (dgm5@st-andrews.ac.uk)
- G. Wadge, Environmental Systems Science Centre, University of Reading, Reading RG6 6AH, UK.